

Reactions of TpRu(CO)(NCMe)(Me) (Tp = Hydridotris(pyrazolyl)borate) with Heteroaromatic Substrates: Stoichiometric and Catalytic C–H Activation

Karl A. Pittard,[†] John P. Lee,[†] Thomas R. Cundari,[‡] T. Brent Gunnoe,^{*,†} and Jeffrey L. Petersen[§]

Department of Chemistry, North Carolina State University, Raleigh, North Carolina 27695-8204, Department of Chemistry, University of North Texas, Box 305070, Denton, Texas 76203-5070, and C. Eugene Bennett Department of Chemistry, West Virginia University, Morgantown, West Virginia 26506-6045

Received July 2, 2004

The Ru(II) complex TpRu(CO)(NCMe)(Me) (Tp = hydridotris(pyrazolyl)borate) initiates carbon–hydrogen bond activation at the 2-position of furan and thiophene to produce methane and TpRu(CO)(NCMe)(aryl) (aryl = 2-furyl or 2-thienyl). Solid-state structures have been determined for TpRu(CO)(NCMe)(2-thienyl) and [TpRu(CO)(μ -C,S-thienyl)]₂. The complex TpRu(CO)(NCMe)(2-furyl) serves as a catalyst for the formation of 2-ethylfuran from ethylene and furan. DFT calculations of the C–H activation of furan by {(Tab)Ru(CO)(Me)} (Tab = tris(azo)borate) indicate that the C–H activation sequence does not proceed through a Ru(IV) oxidative addition intermediate.

Introduction

Transition metal-mediated C–H activation holds promise for the preparation of functionalized products from readily available starting materials. Although significant attention has been focused on systems capable of hydrocarbon C–H functionalization,^{1–7} the design of catalysts for the selective transformation of substrates that contain heteroatomic functionality is also of importance. While multiple studies of metal-mediated activation of heteroaromatic compounds have been directed toward hydrodesulfurization (HDS), hydrodenitrogenation (HDN), and hydrodeoxygenation (HDO) processes,^{8–11} catalytic transformations of C–H bonds of heteroaromatic substrates would provide potentially useful synthetic sequences due to the prevalence of heteroaromatic fragments in compounds of biological interest.

Although five-membered heteroaromatic compounds (e.g., pyrroles, furans, and thiophenes) undergo electrophilic substitutions at the α -position, such reactions are limited to a relatively narrow range of substrates.¹² Stoichiometric transformations of heteroaromatic compounds that are mediated by transition metals include nucleophilic substitutions of *N*-bound and pentahapto-coordinated pyrrolys of Re or Ru complexes.^{13,14} In addition, Harman et al. have incorporated the prolific π -base pentaammineosmium(II) as well as Re(I) systems to bind and activate heteroaromatic compounds toward electrophilic addition.^{15–18} Catalytic transformations of C–H bonds of heteroaromatic compounds are relatively rare. Rh-catalyzed annulations of imidazoles with tethered olefins and furan addition to acetylenes have been reported.^{19–21} Ruthenium catalysts have been used to produce 2-alkyl and 2-alkenyl pyridines as well as for carbonylation reactions of aza-heterocycles.^{22–27} Pd(II)

* To whom correspondence should be addressed. E-mail: brent_gunnoe@ncsu.edu.

[†] North Carolina State University.

[‡] University of North Texas.

[§] West Virginia University.

- (1) Shilov, A. E.; Shul'pin, G. B. *Chem. Rev.* **1997**, *97*, 2879–2932.
- (2) Davies, J. A.; Watson, P. L.; Liebman, J. F.; Greenberg, A. *Selective Hydrocarbon Activation*; VCH: New York, 1990.
- (3) Crabtree, R. H. *J. Chem. Soc., Dalton Trans.* **2001**, 2437–2450.
- (4) Stahl, S. S.; Labinger, J. A.; Bercaw, J. E. *Angew. Chem., Int. Ed.* **1998**, *37*, 2180–2192.
- (5) Arndtsen, B. A.; Bergman, R. G.; Mobley, T. A.; Peterson, T. H. *Acc. Chem. Res.* **1995**, *28*, 154–162.
- (6) Jones, W. D.; Feher, F. J. *Acc. Chem. Res.* **1989**, *22*, 91–100.
- (7) Jia, C.; Kitamura, T.; Fujiwara, Y. *Acc. Chem. Res.* **2001**, *34*, 633–639.
- (8) Angelici, R. J. *Polyhedron* **1997**, *16*, 3073–3088.
- (9) Angelici, R. J. *Acc. Chem. Res.* **1988**, *21*, 387–394.
- (10) Weller, K. J.; Fox, P. A.; Gray, S. D.; Wigley, D. E. *Polyhedron* **1997**, *16*, 3139–3163.
- (11) Jones, W. D.; Vivic, D. A.; Chin, R. M.; Roache, J. H.; Myers, A. W. *Polyhedron* **1997**, *16*, 3115–3128.

(12) Gupta, R. R.; Kumar, M.; Gupta, V. *Heterocyclic Chemistry: II: Five-Membered Heterocycles*; Springer: Berlin, 1999; Vol. 2.

(13) DuBois, M. R.; Parker, K. G.; Ohman, C.; Noll, B. C. *Organometallics* **1997**, *16*, 2325–2334.

(14) DuBois, M. R.; Vasquez, L. D.; Peshlherbe, L.; Noll, B. C. *Organometallics* **1999**, *18*, 2230–2240.

(15) Harman, W. D. *Chem. Rev.* **1997**, *97*, 1953–1978.

(16) Friedman, L. A.; Sabat, M.; Harman, W. D. *J. Am. Chem. Soc.* **2002**, *124*, 7395–7404.

(17) Friedman, L. A.; Harman, W. D. *J. Am. Chem. Soc.* **2001**, *123*, 8967–8973.

(18) Brooks, B. C.; Gunnoe, T. B.; Harman, W. D. *Coord. Chem. Rev.* **2000**, *206–207*, 3–61.

(19) Tan, K. L.; Bergman, R. G.; Ellman, J. A. *J. Am. Chem. Soc.* **2001**, *123*, 2685–2686.

(20) Hong, P.; Cho, B.-R.; Yamazaki, H. *Chem. Lett.* **1980**, 507–510.

(21) Kakiuchi, F.; Yamamoto, Y.; Chatani, N.; Murai, S. *Chem. Lett.* **1995**, 681–682.

(22) Jordan, R. F.; Taylor, D. F. *J. Am. Chem. Soc.* **1989**, *111*, 778–779.

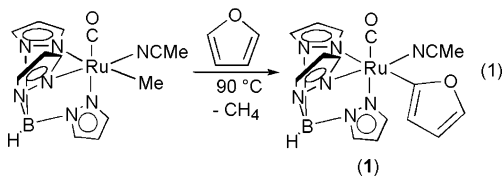
(23) Murakami, M.; Hori, S. *J. Am. Chem. Soc.* **2003**, *125*, 4720–4721.

serves as a catalyst for arylation at all three positions of pyrrole substrates as well as a catalyst for the oxidative coupling of 2-methylfuran and acrylates.^{28,29}

Our group has recently reported that $\text{TpRu}(\text{CO})(\text{NCMe})(\text{R})$ (Tp = hydridotris(pyrazolyl)borate; R = Me or Ph) catalyzes the addition of arene C–H bonds across C=C bonds of olefins,³⁰ and the closely related complex $\text{TpRu}(\text{PPh}_3)(\text{NCMe})\text{H}$ has been reported to activate C–H bonds.³¹ We have extended studies to reactions of $\text{TpRu}(\text{CO})(\text{NCMe})(\text{Me})$ with heteroaromatic substrates and report herein the initial details of these transformations.

Results and Discussion

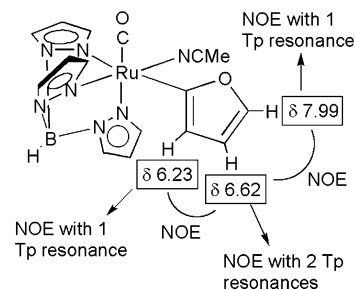
$\text{TpRu}(\text{CO})(\text{NCMe})(\text{Me})$ reacts with furan at 90 °C to yield $\text{TpRu}(\text{CO})(\text{NCMe})(2\text{-furyl})$ (**1**) and methane (eq 1).



The formation of methane has been confirmed by GC–MS analysis of the headspace of a reaction in a gastight NMR tube. Although only isolated in 60% yield after workup, ^1H NMR spectroscopy of the crude reaction mixture reveals that complex **1** is produced in nearly quantitative yield. The C–H activation of furan is regioselective, and ^1H NMR, ^{13}C NMR, homonuclear decoupling, and NOE experiments are consistent with regioselective attack at the 2-position. For example, the chemical shifts (^1H NMR) of complex **1** indicate one downfield resonance and two upfield resonances due to the furyl ligand (7.99, 6.62, and 6.23 ppm) that are consistent with a single α -proton and two β -protons. The ^{13}C NMR spectrum of **1** reveals two resonances at 114.8 and 109.6 ppm that are consistent with *unsubstituted* C–H bonds at the β -position, while the α -carbons resonate at approximately 135 ppm (consistent with an unsubstituted C–H moiety) and 178.8 ppm.

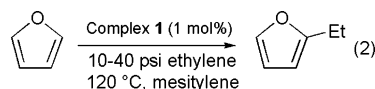
To confirm the regioselectivity of the C–H activation, NOE experiments were performed. Observed enhancements of the 2-furyl ligand are depicted in Chart 1. Most importantly, the resonance at 6.62 ppm (β -position) shows NOEs with the other two furyl resonances. In the case of ruthenium substitution at the 3-position, irradiation of the β -proton would be expected to yield a NOE with a single furyl resonance. Likewise, a 3-furyl ligand would produce a resonance for an α -proton that

Chart 1. Observed NOEs for the 2-Furyl Ligand of $\text{TpRu}(\text{CO})(\text{NCMe})(2\text{-furyl})$ (**1**)



would not be anticipated to exhibit a NOE with either of the remaining two resonances of the furyl ligand. Metal-mediated C–H activations at the 2-position of furan have been reported for Rh and W complexes.^{32–34} In addition, Komiya et al. have reported C–H oxidative addition of furan to an Fe(0) complex in which the regioselectivity was not conclusively determined.³⁵ A binuclear iridium complex has been reported to activate furan to give a 5:2 mixture of 2-furyl and 3-furyl complexes.³⁶ Heating (90 °C) complex **1** with excess furan for 144 h does not result in observable isomerization to the 3-furyl complex.

We have previously reported that the phenyl complex $\text{TpRu}(\text{CO})(\text{Ph})(\text{NCMe})$ serves as a catalyst for the hydroarylation of olefins.³⁰ The combination of furan and 1 mol % of complex **1** (based on furan) in mesitylene at 120 °C under low ethylene pressure (10–40 psi) results in the catalytic production of 2-ethylfuran (eq 2), and



optimal conditions allow approximately 17 catalytic turnovers after 24 h (after which time the catalyst activity decreases). This transformation demonstrates the feasibility of Ru(II)-mediated olefin hydroarylation using heteroaromatic substrates. Although quantitative rate data have not been acquired, higher ethylene pressures result in an increased production of 2-ethylfuran after 24 h of reaction. For example, 9 turnovers are observed after 24 h of reaction at 10 psi of ethylene, 15 turnovers are observed at 30 psi of ethylene, and 17 turnovers are observed using 40 psi of ethylene.

The reaction of $\text{TpRu}(\text{CO})(\text{NCMe})(\text{Me})$ with thiophene produces $\text{TpRu}(\text{CO})(\text{NCMe})(2\text{-thienyl})$ (**2**) and methane after approximately 19 h at 90 °C (Scheme 1). Analyzing the reaction mixture by NMR spectroscopy after 4 h reveals the presence of reaction intermediates. Although products of thiophene/NCMe exchange are likely candidates for reaction intermediates, we have been unable to separate and characterize these species. The reversible formation of metallacycles that result from thiophene

(24) Chatani, N.; Fukuyama, T.; Kakiuchi, F.; Murai, S. *J. Am. Chem. Soc.* **1996**, *118*, 493–494.

(25) Chatani, N.; Ie, Y.; Kakiuchi, F.; Murai, S. *J. Org. Chem.* **1997**, *62*, 2604–2610.

(26) Fukuyama, T.; Chatani, N.; Tatsumi, J.; Kakiuchi, F.; Murai, S. *J. Am. Chem. Soc.* **1998**, *120*, 11522–11523.

(27) Moore, E. J.; Pretzer, W. R.; O'Connell, T. J.; Harris, J.; LaBounty, L.; Chou, L.; Grimmer, S. S. *J. Am. Chem. Soc.* **1992**, *114*, 5888–5890.

(28) Sezen, B.; Sames, D. *J. Am. Chem. Soc.* **2003**, *125*, 5274–5275.

(29) Tsuji, J.; Nagashima, H. *Tetrahedron* **1984**, *40*, 2699–2702.

(30) Lail, M.; Arrowood, B. N.; Gunnoe, T. B. *J. Am. Chem. Soc.* **2003**, *125*, 7506–7507.

(31) Ng, S. M.; Lam, W. H.; Mak, C. C.; Tsang, C. W.; Jia, G.; Lin, Z.; Lau, C. P. *Organometallics* **2003**, *22*, 641–651.

(32) Selnau, H. E.; Merola, J. S. *Organometallics* **1993**, *12*, 1583–1591.

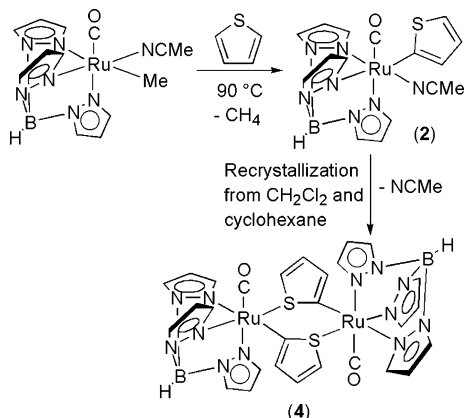
(33) Jones, W. D.; Dong, L.; Myers, A. W. *Organometallics* **1995**, *14*, 855–861.

(34) Samat, A.; Sala-Pala, J.; Guglielmetti, R.; Guerchais, J. *Nouv. J. Chem.* **1978**, *2*, 13–14.

(35) Morikita, T.; Hirano, M.; Sasaki, A.; Komiya, S. *Inorg. Chim. Acta* **1999**, *291*, 341–354.

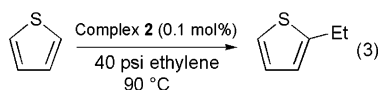
(36) Fujita, K.-i.; Nakaguma, H.; Hamada, T.; Yamaguchi, R. *J. Am. Chem. Soc.* **2003**, *125*, 12368–12369.

Scheme 1. Reaction of TpRu(CO)(NCMe)(Me) with Thiophene Yields TpRu(CO)(NCMe)(2-thienyl) (2)



ring-opening is also possible.³⁷ After extended heating, ¹H NMR spectroscopy indicates that all TpRu intermediates cleanly convert to complex **2**. The ¹H NMR spectrum of complex **2** reveals resonances at 7.25, 6.97, and 6.57 ppm due to the 2-thienyl ligand. Similar to complex **1**, NOE experiments are consistent with a 2-substituted heterocycle (see Supporting Information). Metal-mediated C–H activation of thiophene has been reported.³⁸

Similar to the catalytic addition of furan to ethylene, complex **2** catalyzes the formation of 2-ethylthiophene from a solution of thiophene and ethylene. For example, a thiophene solution of **2** (0.1 mol % versus thiophene) with 40 psi of ethylene pressure at 90 °C produces 2-ethylthiophene (eq 3). A total of 3 catalytic turnovers are observed after 12 h of reaction. The formation of additional 2-ethylthiophene is not observed after 12 h of catalysis.



The addition of HCl to complex **2** ultimately results in the production of free thiophene and a single TpRu product whose ¹H NMR spectrum is consistent with TpRu(CO)(NCMe)(Cl) (Scheme 2). TpRu(CO)(NCMe)(Cl) has been independently prepared by reaction of TpRu(CO)(NCMe)(Me) with HCl (Scheme 2; see Supporting Information for full details). Performing the HCl addition to TpRu(CO)(NCMe)(2-thienyl) (**2**) at –65 °C reveals a kinetic product whose ¹H NMR spectrum is consistent with [TpRu(CO)(NCMe)(S-thiophene)](Cl) (**3**). Warming the CD₂Cl₂ solution to room temperature results in the observation of free thiophene and TpRu(CO)(NCMe)(Cl).

Layering of a methylene chloride solution of **2** with hexane resulted in the growth of crystals, and the structure of complex **2** has been confirmed by a solid-state single-crystal X-ray diffraction study (Figure 1). Data collection parameters are listed in Table 1. Similar to the solid-state structure of Cp*Rh(PMe₃)(Cl)(2-thi-

Scheme 2. Reaction of TpRu(CO)(NCMe)(2-thienyl) (2) with HCl (RT = room temperature)

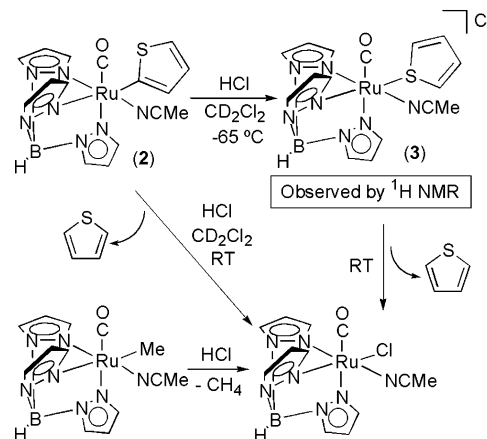


Table 1. Selected Crystallographic Data and Collection Parameters for TpRu(CO)(NCMe)(2-thienyl) (2) and [TpRu(CO)(μ-C,S-2-thienyl)]₂ (4)

	2	4
empirical formula	C ₁₆ H ₁₆ BN ₇ ORuS	C ₁₄ H ₁₃ BN ₆ ORuS
fw	466.30	425.24
cryst syst	monoclinic	triclinic
space group	P2 ₁ /n	P1̄
a, Å	10.5469(9)	8.911(1)
b, Å	12.1519(11)	9.790(1)
c, Å	15.5119(13)	10.200(2)
α, deg		73.405(3)
β, deg	104.698(2)	77.475(3)
γ, deg		78.396(3)
V (Å ³)	1923.0(3)	823.1(2)
Z	4	2
D _{calcd} , g cm ⁻³	1.611	1.716
R1, wR2 (I > 2σ(I))	0.0321, 0.0827	0.0436, 0.1021
GOF	1.037	1.015

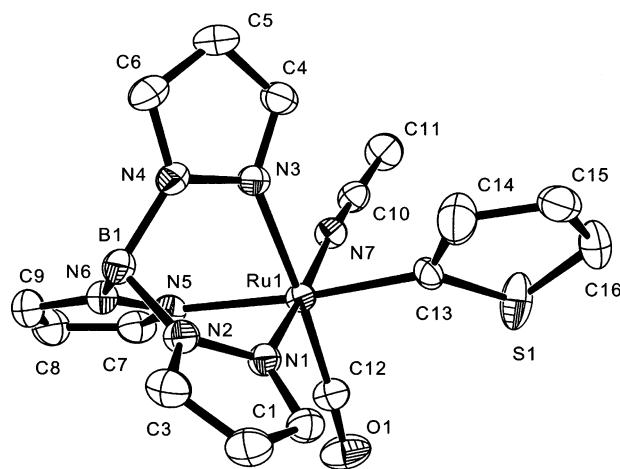


Figure 1. ORTEP of TpRu(CO)(NCMe)(2-thienyl) (**2**) (30% probability). Selected bond distances (Å): Ru–N7 2.029(1), Ru–C13 2.072(2), Ru–N1 2.062(1), Ru–N3 2.141(1), Ru–N5 2.151(1), Ru–C12 1.833(1), N7–C10 1.126(2), S1–C13 1.660(2). Selected bond angles (deg): Ru–C13–S1 125.33(11), C14–C13–S1 108.35(16), Ru–C12–O1 175.98(12).

enyl),³⁹ the 2-thienyl ligand exhibits a 70:30 two-site disorder with the two orientations of the ring differing

(37) Myers, A. W.; Jones, W. D. *Organometallics* **1996**, *13*, 2905–2917.

(38) Bianchini, C.; Casares, J. A.; Osman, R.; Pattison, D. I.; Peruzzini, M.; Perutz, R. N.; Zanobini, F. *Organometallics* **1997**, *16*, 4611–4619, and references therein.

(39) Dong, L.; Duckett, S. B.; Ohman, K. F.; Jones, W. D. *J. Am. Chem. Soc.* **1992**, *114*, 151–160.

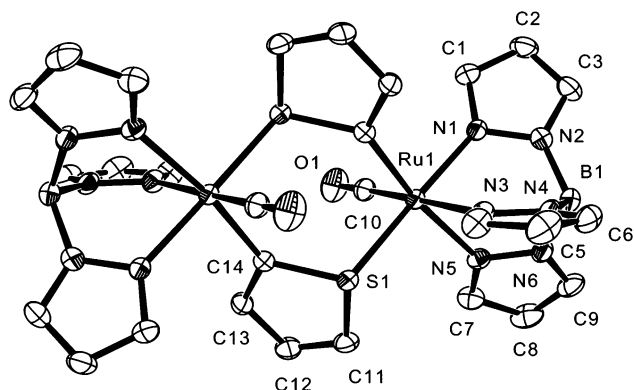
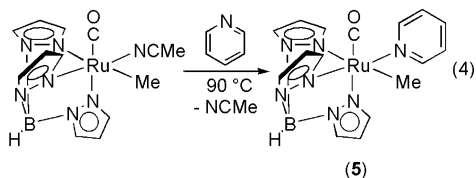


Figure 2. ORTEP of $[\text{TpRu}(\text{CO})(\mu\text{-C,S-thienyl})_2]$ (**4**) (30% probability). Selected bond distances (Å): Ru–S1 2.365(1), Ru–C10 1.824(4), Ru–C14' 2.043(4), Ru–N1 2.076(3), Ru–N3 2.139(3), Ru–N5 2.164(3), S1–C14 1.767(4), C10–O1 1.154(5). Selected bond angles (deg): Ru–S1–C14 110.89(11), C14–S1–C11 94.3(2).

by an approximately 180° rotation about the Ru–C(13) bond. For each of the planar five-membered rings, the S–C(13) bond distance was refined using a restraint of 1.68 Å, the C(14)–C(15) bond distance using a restraint of 1.45 Å, and the C(13)–C(14) and C(15)–C(16) bond distances with restraints of 1.38 Å. The structure confirms the proposed regioselective C–H activation at the 2-position of thiophene.

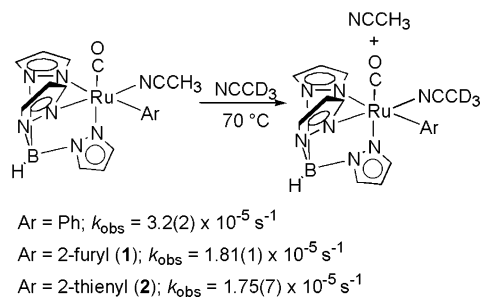
In contrast to recrystallization from methylene chloride/hexane, the recrystallization of complex **2** from methylene chloride/cyclohexane (over a period of approximately two weeks) yields the binuclear complex $[\text{TpRu}(\text{CO})(\mu\text{-C,S-thienyl})_2]$ (**4**) (Scheme 1). Thus, the coordinatively unsaturated species $\{\text{TpRu}(\text{CO})(2\text{-thienyl})\}$ is likely trapped by the sulfur atom of the 2-thienyl ligand of a second Ru complex. Complex **4** was only characterized by a single-crystal X-ray diffraction study (Figure 2). Data collection parameters are listed in Table 1. The two symmetry equivalent Ru fragments are approximately octahedral and are bridged by two $\mu\text{-C,S-2-thienyl}$ ligands. The geometry of the thienyl sulfur atom is pyramidal with the bond angles summing to $316.83(18)^\circ$. The Ru–S bond distance of 2.365(1) Å is similar to other Ru(II) thiophene complexes.⁴⁰

The reaction of pyridine with $\text{TpRu}(\text{CO})(\text{NCMe})(\text{Me})$ at 90°C forms the product from nitrile/pyridine ligand exchange $\text{TpRu}(\text{CO})(\text{N-py})(\text{Me})$ (**5**) (py = pyridine; eq 4).



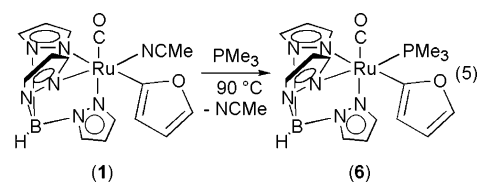
The ^1H NMR spectrum of **5** reveals three resonances due to the five hydrogen atoms of pyridine. The ortho and meta hydrogen atoms are likely equivalent due to rapid rotation about the Ru–N(pyridine) bond. Access to a stable coordination mode of pyridine renders subsequent C–H activation more difficult compared with the reaction of $\text{TpRu}(\text{CO})(\text{NCMe})(\text{Me})$ with furan; however, at elevated temperature (115°C) complex **5**

Scheme 3. Nitrile Exchange Is Observed for $\text{TpRu}(\text{CO})(\text{NCMe})(\text{Ar})$ (Ar = phenyl, 2-furyl, or 2-thienyl) under Pseudo-First-Order Conditions ($[\text{Ru}] = 0.072\text{ M}$)



undergoes slow reaction, requiring approximately 7 days to reach completion. The final product mixture is complex and contains multiple TpRu systems. Column chromatography allows the isolation of a complex whose ^1H NMR and IR spectra are consistent with $\text{TpRu}(\text{CO})(\text{NCMe})(2\text{-pyridyl})$ (see Supporting Information). The production of the 2-pyridyl complex in low yield likely indicates that pyridine C–H activation is not regioselective or that the complex $\text{TpRu}(\text{CO})(\text{NCMe})(2\text{-pyridyl})$ is not stable under the forcing conditions required to achieve C–H activation of pyridine.

Exchange of Acetonitrile for $\text{TpRu}(\text{CO})(\text{NCMe})(\text{Ar})$ Complexes. The acetonitrile ligands of $\text{TpRu}(\text{CO})(\text{NCMe})(\text{aryl})$ (aryl = 2-thienyl, 2-furyl, or phenyl) complexes are labile, as evidenced by the exchange of bound acetonitrile with free NCCD_3 (Scheme 3). The rates of nitrile exchange for the 2-furyl and 2-thienyl complexes are statistically identical. Nitrile exchange for $\text{TpRu}(\text{CO})(\text{NCMe})(\text{Ph})$ is approximately 1.8 times more rapid than the 2-furyl/2-thienyl complexes **1** and **2**. The labile nature of the nitrile ligand allows ligand exchange reactions. For example, $\text{TpRu}(\text{CO})(\text{NCMe})(2\text{-furyl})$ (**1**) reacts with PMe_3 to produce $\text{TpRu}(\text{CO})(\text{PMe}_3)(2\text{-furyl})$ (**6**) (eq 5).



Mechanism of C–H Activation. Late transition metal centers in low oxidation states have been demonstrated to cleave C–H bonds via insertion of the metal into the C–H bond with a formal +2 increase in metal oxidation state (i.e., oxidative addition). Of particular relevance here are C–H activations by d^6 metal centers that are isoelectronic to $\text{TpRu}(\text{CO})(\text{NCMe})(\text{R})$. For example, Bergman et al. have reported that $\text{Cp}^*(\text{PMe}_3)\text{-Ir}^{\text{III}}(\text{Me})(\text{OTf})$ and $[\text{Cp}^*(\text{PMe}_3)\text{Ir}^{\text{III}}(\text{Me})(\text{CH}_2\text{Cl}_2)][\text{BAR}'_4]$, Ar' = 3,5-(CF_3) $_2\text{C}_6\text{H}_3$, can selectively activate the C–H bonds of a range of substrates below room temperature.^{41,42} In addition, Ir(III) complexes with oxygen-donor ligands can *catalytically* add arene C–H bonds across unsaturated carbon–carbon bonds as well as

(40) Benson, J. W.; Angelici, R. J. *Organometallics* **1992**, *11*, 922–927.

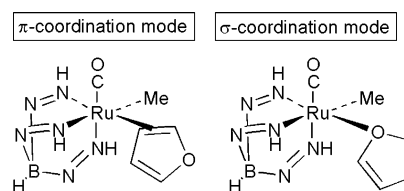
(41) Arndtsen, B. A.; Bergman, R. G. *Science* **1995**, *270*, 1970–1972.
 (42) Burger, P.; Bergman, R. G. *J. Am. Chem. Soc.* **1993**, *115*, 10462–10463.

initiate alkane C–H activation.^{43–46} Substantial speculation has been focused on the mechanism of the C–H bond breaking step for the Ir(III) systems.^{47–51} An oxidative addition mechanism is consistent with known pathways for late transition metal complexes but would involve an atypically high Ir(V) oxidation state. An alternative pathway is σ -bond metathesis;^{52–56} however, to our knowledge, σ -bond metathesis mechanisms for C–H activation have not been definitively demonstrated for late transition metal systems. Hartwig et al. have demonstrated that Ru(II) activation of B–H bonds likely occurs through a σ -bond metathesis mechanism.⁵⁷

To help discern the likely mechanism of C–H activation by the fragment $\{\text{TpRu}(\text{CO})(\text{Me})\}$, B3LYP/SBK(d) calculations were employed. As a model of the full (tris-pyrazolyl)borate (Tp) ligand, the tris(azo)borate (Tab) ligand, $[\text{HB}(-\text{N}=\text{NH})_3]^-$, was used. In previous research, Tab was shown to faithfully reproduce the structure and energetics of the full Tp models for C–H activation potential energy surfaces.⁵⁸ Calculations were performed with furan as the representative reactant.

Experimental kinetic studies suggest that C–H activation of benzene by $\text{TpRu}(\text{CO})(\text{NCMe})(\text{Me})$ proceeds through initial acetonitrile/benzene ligand exchange,³⁰ and we considered an analogous initial step for the C–H activation of furan. Two coordination modes were considered for the interaction of ruthenium and furan: σ (η^1 -coordination through oxygen) and π (η^2 -coordination through C=C bond; Scheme 4). Both coordination modes were constructed and evaluated. The π -coordination mode is preferred relative to the corresponding σ -isomer by 3.8 kcal/mol. The calculated free energies for π - versus σ -coordination are consistent with experimental observations since η^2 -coordinated furan complexes have been isolated, while, to our knowledge, examples of isolable η^1 -O-bound furan systems are unknown.^{15,17,59,60}

Scheme 4. Two Coordination Modes Considered for Furan with the π -Coordination Mode Calculated to Be Favored versus the σ -Coordination Mode



Hence, in the discussion below, $(\text{Tab})\text{Ru}(\text{Me})(\text{C}_4\text{H}_4\text{O})(\text{CO})$ refers exclusively to the more stable π -coordinated isomer.

Studies of the overall process of furan C–H activation and methane release were broken down into three steps: (1) furan coordination, (2) C–H activation of furan, and (3) coordination of the acetonitrile model $\text{N}\equiv\text{CH}$ to complete the reaction. The resulting energetic parameters are depicted in Scheme 5 (optimized geometries for the reaction intermediates are illustrated in the Supporting Information). The displacement of $\text{N}\equiv\text{CH}$ by $\text{C}_4\text{H}_4\text{O}$ is calculated to be *endergonic* by 14.4 kcal/mol. Given a calculated free energy of binding of $\text{N}\equiv\text{CH}$ to $\{(\text{Tab})\text{Ru}(\text{Me})(\text{CO})\}$ of 14.9 kcal/mol, this corresponds to a binding free energy of furan to $(\text{Tab})\text{Ru}(\text{Me})(\text{CO})$ of -0.5 kcal/mol. Weak binding is expected for dihapto-ligation of a π -heteroatomic system to a closed-shell, $d^6 \text{ML}_5$ fragment. The C–H activation step is *exergonic* by 13.4 kcal/mol with a calculated free energy of activation of 17.4 kcal/mol. The overall reaction sequence $\text{Ru}(\text{Me})(\text{CO})(\text{NCH}) + \text{C}_4\text{H}_4\text{O} \rightarrow \text{Ru}(\text{Me})(\text{CO})(\text{NCH}) + \text{C}_4\text{H}_3\text{O}(\text{CO})(\text{NCH}) + \text{CH}_4$ is *exergonic* by 10.3 kcal/mol. Assuming that the change in entropy for the overall C–H activation is negligible, the C–H bond dissociation energies of methane (104 kcal/mol) and furan (118 kcal/mol) indicate that the Ru–2-furyl bond is stronger than the Ru– CH_3 bond by approximately 24 kcal/mol.⁶¹

To explore the C–H activation step, a variety of calculations were performed using furan as a model substrate (Scheme 6). Several pathways were investigated including oxidative addition of a furan C–H bond to the Ru of $\{(\text{Tab})\text{Ru}(\text{CO})\text{Me}\}$ (**A**), oxidative addition of a methane C–H bond to the Ru of $\{(\text{Tab})\text{Ru}(\text{CO})(2\text{-furyl})\}$ (**B**), and nonoxidative addition at the 2-position C–H bond of furan to the Ru– CH_3 bond of $\{(\text{Tab})\text{Ru}(\text{CO})(\text{Me})\}$ (**C**). Multiple starting geometries were investigated for each of the proposed transition states. In all cases, the transition states collapsed to **C** (i.e., the nonoxidative addition transition state). The identity of the transition state was confirmed by calculation of the intrinsic reaction coordinate along the imaginary frequency, the primary motion of which corresponded to transfer of the transannular hydrogen from the methyl to the furyl carbon.

The calculated transition-state geometry for C–H activation of furan and pertinent metric data are depicted in Figure 3. The near equivalent C–H distances between the methyl and furyl ligands and the hydrogen atom undergoing transfer are indicative of a transition state that is roughly intermediate between reactants and products and hence neither early nor late.

(43) Matsumoto, T.; Taube, D. J.; Periana, R. A.; Taube, H.; Yoshida, H. *J. Am. Chem. Soc.* **2000**, *122*, 7414–7415.

(44) Periana, R. A.; Liu, X. Y.; Bhalla, G. *Chem. Commun.* **2002**, *24*, 3000–3001.

(45) Matsumoto, T.; Periana, R. A.; Taube, D. J.; Yoshida, H. *J. Mol. Catal. A: Chem.* **2002**, *180*, 1–18.

(46) Wong-Foy, A. G.; Bhalla, G.; Liu, X. Y.; Periana, R. A. *J. Am. Chem. Soc.* **2003**, *125*, 14292–14293.

(47) Tellers, D. M.; Yung, C. M.; Arndtsen, B. A.; Adamson, D. R.; Bergman, R. G. *J. Am. Chem. Soc.* **2002**, *124*, 1400–1410.

(48) Alaimo, P. J.; Bergman, R. G. *Organometallics* **1999**, *18*, 2707–2717.

(49) Hinderling, C.; Feichtinger, D.; Plattner, D. A.; Chen, P. *J. Am. Chem. Soc.* **1997**, *119*, 10793–10804.

(50) Su, M.-D.; Chu, S.-Y. *J. Am. Chem. Soc.* **1997**, *119*, 5373–5383.

(51) Strout, D. L.; Zoric, S.; Niu, S.; Hall, M. B. *J. Am. Chem. Soc.* **1996**, *118*, 6068–6069.

(52) Rothwell, I. P. In *Selective Hydrocarbon Activation: Principles and Progress*; Davies, J. A., Watson, P. L., Greenberg, A., Liebman, J. F., Eds.; VCH Publishers: New York, 1990; pp 43–78.

(53) Watson, P. L. In *Selective Hydrocarbon Activation: Principles and Progress*; Davies, J. A., Watson, P. L., Liebman, J. F., Greenberg, A., Eds.; VCH Publishers: New York, 1990; pp 79–112.

(54) Watson, P. L. *J. Am. Chem. Soc.* **1983**, *105*, 6491–6493.

(55) Thompson, M. E.; Baxter, S. M.; Bulls, A. R.; Burger, B. J.; Nolan, M. C.; Santarsiero, B. D.; Schaefer, W. P.; Bercaw, J. E. *J. Am. Chem. Soc.* **1987**, *109*, 203–219.

(56) Rothwell, I. P. *Polyhedron* **1985**, *4*, 177–200.

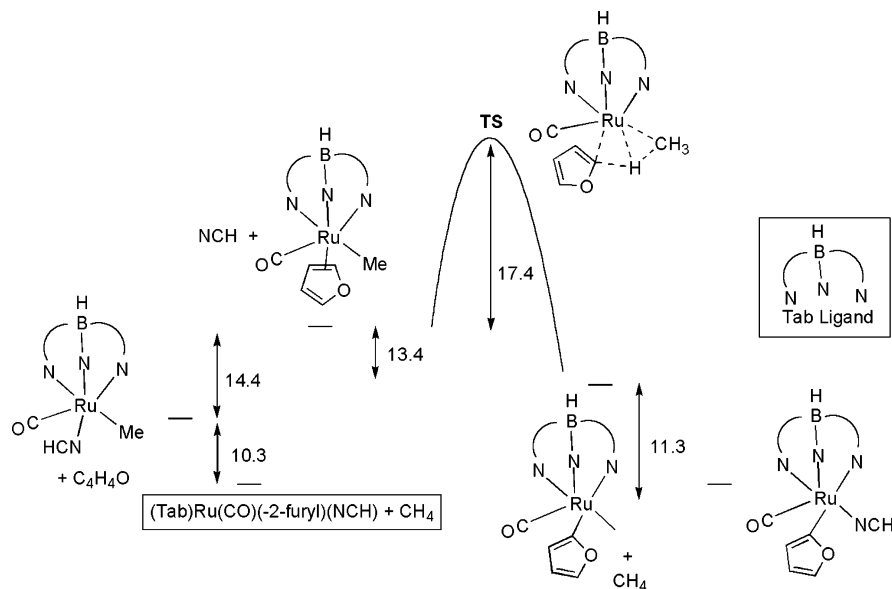
(57) Hartwig, J. F.; Bhandari, S.; Rablen, P. R. *J. Am. Chem. Soc.* **1994**, *116*, 1839–1844.

(58) Bergman, R. G.; Cundari, T. R.; Gillespie, A. M.; Gunnoe, T. B.; Harman, W. D.; Klinckman, T. R.; Temple, M. D.; White, D. P. *Organometallics* **2003**, *22*, 2331–2337.

(59) Gunnoe, T. B.; Sabat, M.; Harman, W. D. *J. Am. Chem. Soc.* **1998**, *120*, 8747–8754.

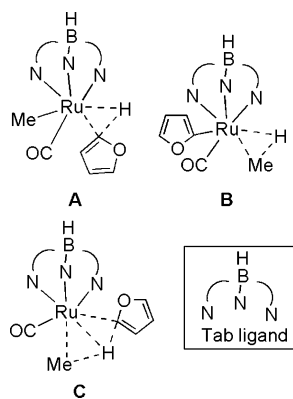
(60) Brooks, B. C.; Chin, R. M.; Harman, W. D. *Organometallics* **1998**, *17*, 4716–4723.

(61) Barckholtz, C.; Barckholtz, T. A.; Hadad, C. M. *J. Am. Chem. Soc.* **1999**, *121*, 491–500.

Scheme 5. B3LYP/SBK-31G(d) Calculated Free Energies (kcal/mol) for the C–H Activation of Furan^a

^a Gibbs free energy of activation; [Ru] = (Tab)Ru.

Scheme 6. Various Pathways for Furan C–H Activation that Were Studied by DFT Calculations



One interesting factor regarding the transition-state geometry is the close metal–transannular hydrogen distance (1.75 Å). Closely related results have been reported from calculations to probe the mechanism of C–H activation for $\text{TpM}(\text{PH}_3)(\text{Me})$ ($\text{M} = \text{Fe}$ or Ru) complexes in which the authors suggested that the reaction pathways are intermediate between oxidative addition and σ -bond metathesis processes.⁶² Computational studies of methane activation by $\text{Pt}(\text{H}_2\text{O})\text{Cl}_2$ indicate a similar four-center transition state with a $\text{Pt}–\text{H}$ bond distance of 1.99 Å.⁶³ Calculations on the transition state of benzene C–H activation by $(\text{acac})_2\text{Ir}(\text{CH}_2\text{CH}_2\text{Ph})$ and $\text{TpRu}(\text{CO})(\text{CH}_2\text{CH}_2\text{Ph})$ reveal an Ir–H bond distance of 1.58 Å and a Ru–H bond distance of 1.61 Å, respectively, and Goddard et al. have differentiated this transition state (in which there is a metal–hydrogen interaction) from a σ -bond metathesis transition state using the label oxidative hydrogen migration.^{64,65}

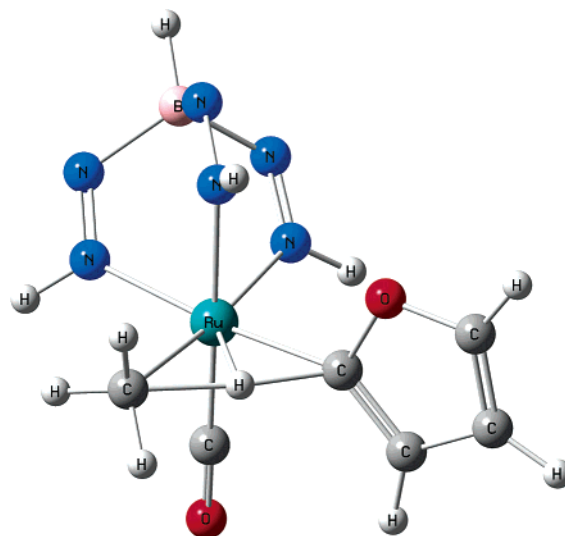


Figure 3. Calculated transition-state geometry for furan C–H activation by $\{(\text{Tab})\text{Ru}(\text{CO})(\text{CH}_3)\}$. Bond lengths for C–H activation active site: $\text{Ru}–\text{C}_{\text{furyl}} = 2.17$ Å; $\text{C}_{\text{furyl}}–\text{H}_t = 1.44$ Å; $\text{H}_t–\text{C}_{\text{methyl}} = 1.54$ Å; $\text{Ru}–\text{C}_{\text{methyl}} = 2.32$ Å; $\text{Ru}–\text{H}_t = 1.75$ Å.

As previously discussed for early transition metal systems,^{55,66,67} for C–H activation that proceeds without an oxidative addition intermediate, a distinction can be made between σ -bond metathesis and electrophilic aromatic substitution. The calculated transition state for furan C–H activation by $\{(\text{Tab})\text{Ru}(\text{CO})(\text{CH}_3)\}$ reveals that the hydrogen atom undergoing transfer to the methyl ligand is out of the aromatic plane (Figure 4). The calculated $\text{Ru}–\text{C}_{\text{furyl}}–\text{H}$ bond angle in the transition state is 53.3° , and the out-of-plane position is consistent with a change in hybridization from sp^2 to sp^3 at the center of C–H activation. The disruption of planarity

(62) Lam, W. H.; Jia, G.; Lin, Z.; Lau, C. P.; Eisenstein, O. *Chem. Eur. J.* **2003**, *9*, 2775–2782.

(63) Siegbahn, P. E. M.; Crabtree, R. H. *J. Am. Chem. Soc.* **1996**, *118*, 4442–4450.

(64) Oxgaard, J.; Muller, R. P.; Goddard, W. A., III; Periana, R. A. *J. Am. Chem. Soc.* **2004**, *126*, 352–363.

(65) Oxgaard, J.; Goddard, W. A., III. *J. Am. Chem. Soc.* **2004**, *126*, 442–443.

(66) Bulls, A. R.; Schaefer, W. P.; Serfas, M.; Bercaw, J. E. *Organometallics* **1987**, *6*, 1219–1226.

(67) Chesnut, R. W.; Jacob, G. G.; Yu, J. S.; Fanwick, P. E.; Rothwell, I. P. *Organometallics* **1991**, *10*, 321–328.

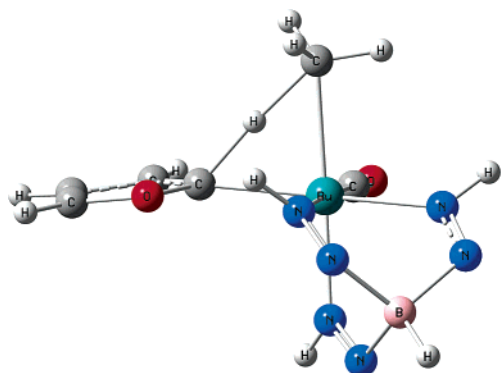
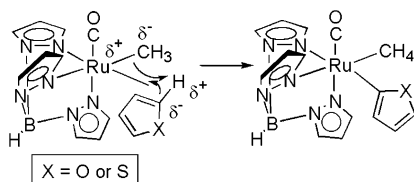


Figure 4. View of calculated transition state for C–H activation of furan that illustrates the “out-of-plane” position of hydrogen atom undergoing transfer.

Scheme 7. Intramolecular Proton Transfer Is Consistent with the Regioselectivity of C–H Activation



and hence aromaticity could reflect a pathway for C–H activation that is related to electrophilic substitution in which the electrophilic Ru(II) center attacks the furan π -system. Alternatively, the out-of-plane hydrogen could reflect progress along the reaction coordinate and incipient Ru–C bond formation.

Given the similar C–H bond dissociation energies at the 2- and 3-position of five-membered heteroaromatic compounds,⁶¹ the regioselective cleavage of the 2-position C–H bonds of thiophene and furan implicates the potential importance of the electrophilic nature of the Ru(II) center. It is known that electrophilic additions to five-membered heteroaromatic compounds occur selectively at the 2-position due to favorable resonance stabilization,¹² and we propose that an electrophilic attack of Ru on the aromatic substrate likely precedes and/or initiates C–H activation, a supposition supported by the calculated positive charge on the furan fragment in (Tp)Ru(Me)(η^2 -C₄H₄O)(CO). Electrophilic addition of Ru(II) would substantially increase the acidity of ring C–H bonds, and subsequent C–H activation through a nonoxidative addition pathway could be viewed as an intramolecular heterolytic process for which the methyl ligand acts as a base to remove a proton from furan or thiophene (Scheme 7). The Ru–H interaction in the calculated transition state likely imparts more hydridic (or, perhaps equally accurate, less acidic) character to the transannular hydrogen; however, the bonding orbitals involving the transannular hydrogen are predominantly Ru in character. The proposed model of the Ru(II)-mediated C–H activation is closely related to that suggested for C–H activation by tungsten and iron boryl complexes.⁶⁸ Selnau and Merola have previously noted that the acidity of C–H bonds may play a role in metal-mediated oxidative addition transformations, al-

though the relative acidity of C–H bonds of “free” heteroaromatic substrates may not be as important as that of substrates that result from electrophilic addition.³² The regioselectivity of furan and thiophene C–H activation by TpRu(CO)(NCMe)(Me) is not conclusive for a nonoxidative addition pathway since identical regioselectivities have been reported for systems that initiate well-defined oxidative addition;^{32,33} however, not all oxidative addition transformations are regioselective, as illustrated by a binuclear iridium system that initiates oxidative addition of furan to produce a 5:2 ratio of 2-furyl and 3-furyl products.³⁶ Even though the regioselectivity for oxidative addition of hydrocarbons is often guided by bond dissociation energies,^{6,69,70} the observation of a final oxidative addition product for heteroaromatic substrates neither precludes the intermediacy of an electrophilic addition product that precedes C–H activation nor rules out the importance of the electrophilic character of the metal center in the overall C–H activation. Thus, even in the absence of a “true” electrophilic addition of Ru(II), the electrophilic nature of the metal center could still serve to guide the regioselectivity.

Summary and Conclusions

The presence of the Tp ligand may predispose the Ru(II) systems {TpRu(CO)(R)} against oxidative addition intermediates given the well-documented predilection against seven-coordinate complexes for complexes that possess Tp or related ligands.⁵⁸ Experimental and computational studies of aromatic C–H activation by the {TpRu(CO)(Me)} fragment are consistent with a nonoxidative addition pathway in which the electrophilic character of Ru(II) may dictate regioselectivity. The potential synthetic advantage of this pathway is the ability to utilize charge localization on aromatic substrates to direct the regioselectivity of C–H activation as demonstrated by the catalytic synthesis of 2-ethylfuran from furan and ethylene.

Experimental Section

General Methods. Unless otherwise noted, all synthetic procedures were performed under a dinitrogen atmosphere using either standard Schlenk line or glovebox techniques. Glovebox atmosphere was maintained at O₂ (g) < 15 ppm for all reactions. Mesitylene was vacuum distilled prior to use. Furan was distilled prior to use. Acetonitrile was distilled over CaH₂. Hexanes, methylene chloride, and tetrahydrofuran were purchased as OptiDry solvents (<50 ppm H₂O) and passed through columns of activated alumina (under nitrogen pressure) prior to use. Decane and 2-ethylfuran were used as received from commercial sources. Ethylene was purchased from National Welders Supply Co. and used as received. CD₃CN, acetone-*d*₆, CD₂Cl₂, benzene-*d*₆, and CDCl₃ were degassed with three freeze–pump–thaw cycles and stored under a dinitrogen atmosphere over 4 Å molecular sieves. ¹H and ¹³C NMR spectra were recorded on a Varian Mercury 300 or 400 MHz spectrometer. NOE experiments were conducted on a Varian Mercury 400 MHz spectrometer using 64 scans with a 1 s mixing time. Gas chromatography was carried out on a Hewlett-Packard 5890 GC equipped with a J&W SE-30 or

(69) Northcutt, T. O.; Wick, D. D.; Vetter, A. J.; Jones, W. D. *J. Am. Chem. Soc.* **2001**, *123*, 7257–7270.

(70) Flood, T. C.; Janak, K. E.; Iimura, M.; Zhen, H. *J. Am. Chem. Soc.* **2000**, *122*, 6783–6784.

(68) Webster, C. E.; Fan, Y.; Hall, M. B.; Kunz, D.; Hartwig, J. F. *J. Am. Chem. Soc.* **2003**, *125*, 858–859.

HP5-MS capillary column, split inlet, and FID detector. Chromatographs were produced using an HP3396 Series II integrator or PE Totalchrome software package. IR spectra were acquired by a Mattson Genesis II FT-IR as thin films on KBr plates or as solutions in KBr solvent cells. $\text{TpRu}(\text{CO})\text{-(NCMe)(Me)}$ and $\text{TpRu}(\text{CO})\text{-(NCMe)(Ph)}$ were prepared according to the published procedures.³⁰

Calculations. Quantum calculations were carried out using the Gaussian 98 package.⁷¹ The B3LYP hybrid functional was employed for all calculations.⁷² Heavy atoms were described with the Stevens relativistic effective core potentials (ECPs) and valence basis sets (VBSs).^{73,74} The valence basis sets of main group elements were augmented with a d polarization function. This ECP/VBS combination, termed SBK(d), has been validated for the calculation of a wide variety of transition metal properties in previous studies.^{58,75,76} All stationary points were fully optimized without symmetry constraint. Several conformations of the different ligands were investigated by torsion about the appropriate metal–ligand bonds; the lowest energy conformers found were used in the analyses given in this paper. The energy Hessian was calculated at all stationary points to characterize them as minima (no imaginary frequencies) or transition states (one and only one imaginary frequency). The quoted energies include zero-point, enthalpy, and entropic corrections determined from unscaled vibrational frequencies calculated at the B3LYP/SBK(d) level of theory. All energetic determinations were done at 298.15 K and 1 atm.

$\text{TpRu}(\text{CO})\text{-(NCMe)(2-furyl)}$ (1). $\text{TpRu}(\text{NCMe})(\text{CO})(\text{CH}_3)$ (0.227 g, 0.570 mmol) was added to a thick-walled glass pressure vessel containing approximately 25 mL of furan. The vessel was sealed, and the reaction mixture was heated in a 90 °C oil bath for 36 h. After cooling the solution to room temperature, all volatiles were removed in vacuo. The resulting pale pink-colored solid was taken up in THF (~2 mL) and precipitated with hexanes (~25 mL). The resulting amorphous solid was collected via filtration and washed with hexanes (2 × 10 mL). The isolated product was dried under reduced pressure to yield a pale pink-colored solid (0.155 g, 60%). IR (KBr): ν_{CO} 1949 cm^{-1} , ν_{CN} 2286 cm^{-1} , ν_{BH} 2484 cm^{-1} . ^1H NMR (C_6D_6 , δ): 7.99 (1H, dd, $J_{\text{HH}} = 1.5$ and 0.6 Hz, α -furyl CH), 7.89, 7.60, 7.43, 7.40, 7.29 (6H, 1:2:1:1:1 integration, each a d, Tp CH 3- or 5-position), 6.62 (1H, dd, $J_{\text{HH}} = 2.7$ and 1.5 Hz, β -unbound of furyl CH), 6.23 (1H, dd, $J_{\text{HH}} = 2.7$ and 0.6 Hz, β -bound of furyl CH), 5.96, 5.67 (3H, 2:1 integration, each a t, Tp CH 4-position), 0.37 (3H, s, NCCH_3). $^{13}\text{C}\{^1\text{H}\}$ NMR (CDCl_3 , δ): 203.9 (CO), 178.8 (ipso-furyl), 145.2, 144.3, 142.4, 142.2 (Tp 3- and 5-position), 135.3, 134.7, 134.5 (α -unbound of furyl and Tp 3- and 5-position), 122.1 (Ru- NCCH_3), 114.8, 109.6 (β -position of furyl), 105.5, 105.2 (Tp 4-position, coincidental overlap of two resonances), 4.3 (Ru- NCCH_3). Anal. Calcd for $\text{C}_{16}\text{H}_{16}\text{BN}_7\text{O}_2\text{Ru}$: C, 42.68; H, 3.58; N, 21.78. Found: C, 42.71;

H, 3.50; N, 21.57. To determine the composition of the crude reaction product, an aliquot of the homogeneous solution was taken prior to workup. The solvent was removed under reduced pressure, and the resulting film was dissolved in C_6D_6 . The entire solid was dissolved to give a homogeneous solution. Complex **1** was the only observable species using ^1H NMR spectroscopy. The NOE data were acquired using a Varian Mercury 400 MHz instrument in C_6D_6 with a mixing time of 1 s and delay time of 25 s.

$\text{TpRu}(\text{CO})\text{-(NCMe)(2-thienyl)}$ (2). A thick-walled glass reaction vessel was charged with $\text{TpRu}(\text{CO})\text{-(NCMe)(Me)}$ (0.243 g, 0.609 mmol) and thiophene (~5 mL). The reaction vessel was heated to 90 °C for 19 h. The reaction solution was then cooled to room temperature, and the volatiles were removed under reduced pressure. The residuals were taken up in methylene chloride, and upon addition of hexanes, a precipitate formed. The resulting beige solid was collected via vacuum filtration and dried under reduced pressure to yield 0.242 g (88%) of product. IR (KBr): ν_{CO} 1946 cm^{-1} , ν_{CN} 2284 cm^{-1} , ν_{BH} 2484 cm^{-1} . ^1H NMR (CD_3CN , δ): 7.86 (1H, d, Tp CH, 3- or 5-position), 7.81 (2H, m, Tp CH, 3- or 5-position), 7.79 (1H, dd, Tp CH 3- or 5-position), 7.47 (1H, d, Tp CH, 3- or 5-position), 7.25 (1H, dd, $J = 5$, 1 Hz, thienyl 2-position CH), 6.97 (1H, dd, $J = 5$, 3 Hz, thienyl 3-position unbound CH), 6.57 (1H, dd, $J = 3$, 1 Hz, thienyl 2-position bound CH), 6.31, 6.25, 6.18 (each 1H, each a t, Tp CH 4-position), 2.33 (3H, s, NCCH_3). $^{13}\text{C}\{^1\text{H}\}$ NMR (CD_3CN , δ): 204.0 (CO), 158.9 (ipso thienyl), 145.7, 142.8, 142.6, 135.6, 135.1, 134.7, 132.5, 127.2, 125.9 (Tp 3- and 5-position or thienyl), 122.5 (Ru- NCCH_3), 105.7, 105.3 (Tp 4-position with overlap of two resonances), 4.4 (Ru- NCCH_3). Anal. Calcd for $\text{C}_{16}\text{H}_{16}\text{BN}_7\text{O}_2\text{RuS}$: C, 41.21; H, 3.46; N, 21.03. Found: C, 40.77; H, 3.52; N, 20.32.

Reaction of $\text{TpRu}(\text{CO})\text{-(NCMe)(2-thienyl)}$ (2) with HCl: Observation of $[\text{TpRu}(\text{CO})\text{-(NCMe)(S-thiophene)]\text{[Cl]}$ (3). Under an atmosphere of dinitrogen, a screw-cap NMR tube was charged with $\text{TpRu}(\text{NCMe})(\text{CO})(2\text{-thienyl})$ (2) (0.020 g) and CD_2Cl_2 (0.6 mL). The solution was cooled to -65 °C, and 1 equiv of HCl (44 μL , 1 M in Et_2O) was added. Upon addition of HCl, a color change from pink to yellow was noted. A ^1H NMR spectrum was acquired of the reaction solution at -65 °C. As detailed below, the spectrum was consistent with the formation of $[\text{TpRu}(\text{NCMe})(\text{CO})(\text{S-thiophene})]\text{[Cl]}$. Upon warming to room temperature, ^1H NMR spectroscopy revealed the formation of $\text{TpRu}(\text{NCMe})(\text{CO})(\text{Cl})$ and free thiophene. The addition of thiophene to the reaction sample confirmed the presence of free thiophene.

$[\text{TpRu}(\text{CO})\text{-(NCMe)(S-thiophene)]\text{[Cl]}$ (3). ^1H NMR (CD_2Cl_2 , δ): 7.93, 7.85 (each 1H, br s, Tp CH 3- and 5-position), 7.72 (3H, m, Tp CH 3- and 5-position), 7.61 (2H, br s, α -thiophene), 7.36 (2H, br s, β -thiophene), 7.05 (1H, br s, Tp CH, 3- and 5-position), 6.39, 6.27, 6.18 (each 1H, br s, Tp CH, 4-position), 2.09 (3H, s, NCCH_3).

$\text{TpRu}(\text{CO})\text{-(Me)(N-pyridine)}$ (5). In a thick-walled glass pressure vessel, $\text{TpRu}(\text{CO})\text{-(NCMe)(CH}_3)$ (0.101 g, 0.256 mmol) was dissolved in pyridine (5 mL). The mixture was heated to 90 °C for 5 h. The reaction solution was then cooled to room temperature and purged into a glovebox, and the volatiles were removed under reduced pressure. The resulting product was precipitated from methylene chloride upon addition of hexanes, and the precipitate was collected by vacuum filtration through a fine-porosity frit. The resulting solid was dried under vacuum to yield a bright yellow product (0.063 g, 56%). IR (KBr): ν_{CO} 1902 cm^{-1} , ν_{BH} 2478 cm^{-1} . ^1H NMR (C_6D_6 , δ): 8.16 (2H, m, pyridine ortho CH), 7.70 (1H, dd, Tp CH, 3- or 5-position), 7.57 (1H, dd, Tp CH 3- and 5-position), 7.51 (1H, dd, Tp CH, 3- and 5-position), 7.43 (1H, dd, Tp CH, 3- and 5-position), 7.12 {2H, s (overlapping doublets), Tp CH, 3- or 5-position}, 6.62 (1H, tt, $J_{\text{HH}} = 7.7$, 1.8 Hz, pyridine para-CH), 6.12 (2H, m, pyridine meta-CH), 5.94 (1H, t, Tp CH 4-position), 5.90 (1H, t, Tp CH 4-position), 5.82 (1H, t, Tp CH, 4-position), 0.89 (3H, s, NCCH_3). $^{13}\text{C}\{^1\text{H}\}$ NMR (C_6D_6 , δ): 209.0 (CO), 155.7, 144.7,

(71) Frisch, M. J.; Trucks, G. W.; Schlegel, H. B.; Scuseria, G. E.; Robb, M. A.; Cheeseman, J. R.; Zakrzewski, V. G.; Montgomery, J. A., Jr.; Stratmann, R. E.; Burant, J. C.; Dapprich, S.; Millam, J. M.; Daniels, A. D.; Kudin, K. N.; Strain, M. C.; Farkas, O.; Tomasi, J.; Barone, V.; Cossi, M.; Cammi, R.; Mennucci, B.; Pomelli, C.; Adamo, C.; Clifford, S.; Ochterski, J.; Petersson, G. A.; Ayala, P. Y.; Cui, Q.; Morokuma, K.; Malick, D. K.; Rabuck, A. D.; Raghavachari, K.; Foresman, J. B.; Cioslowski, J.; Ortiz, J. V.; Baboul, A. G.; Stefanov, B. B.; Liu, G.; Liashenko, A.; Piskorz, P.; Komaromi, I.; Gomperts, R.; Martin, R. L.; Fox, D. J.; Keith, T.; Al-Laham, M. A.; Peng, C. Y.; Nanayakkara, A.; Challacombe, M.; Gill, P. M. W.; Johnson, B.; Chen, W.; Wong, M. W.; Andres, J. L.; Gonzalez, C.; Head-Gordon, M.; Replogle, E. S.; Pople, J. A. *Gaussian 98, Revision A.9*; Gaussian Inc.: Pittsburgh, PA, 1998.

(72) Becke, A. D. *J. Chem. Phys.* **1993**, *98*, 5648–5652.

(73) Stevens, W. J.; Basch, H.; Krauss, M. *J. Chem. Phys.* **1984**, *81*, 6026–6033.

(74) Stevens, W. J.; Krauss, M.; Basch, H.; Jasien, P. G. *Can. J. Chem.* **1992**, *70*, 612–613.

(75) Cundari, T. R.; Klinckman, T. R.; Wolczanski, P. T. *J. Am. Chem. Soc.* **2002**, *124*, 1481–1487.

(76) Holland, P. L.; Cundari, T. R.; Perez, L. L.; Eckert, N. A.; Lachicotte, R. J. *J. Am. Chem. Soc.* **2002**, *124*, 14416–14424.

142.7, 140.8, 135.6, 135.1, 135.0, 134.6, 124.0 (Tp 3- and 5-position, pyridine and Ru-NCMe) 106.5, 106.3, 106.2 (Tp 4-position), -4.1 (Ru-CH₃). Anal. Calcd for C₁₆H₁₈BN₇ORu: C, 44.05; H, 4.16; N, 22.47. Found: C, 44.12; H, 4.22, N, 22.16.

TpRu(CO)(PMe₃)(2-furyl) (6). A thick-walled pressure tube was charged with [TpRu(NCMe)(CO)(2-furyl)] (1) (0.228 g, 0.051 mmol) and THF (~8 mL). To the orange-yellow solution was added PMe₃ (80 μL, 0.08 mmol), and the mixture was heated at 90 °C for 20 h. The solvent was removed in vacuo, and the resulting solid was stirred in hexanes. The pale yellow solid was collected after vacuum filtration and dried (0.099 g, 38%). IR (KBr): ν_{CO} 1943 cm⁻¹. ¹H NMR (CDCl₃, δ): 7.74 (1H, α-furyl CH, d, ³J_{HH} = 1.5 Hz), 7.69, 7.65, 7.58, 7.55, 7.42 (6H, 2:1:1:1:1 integration, each a d, Tp CH 3- or 5-position), 6.26 (1H, β-furyl CH unbound, dd, ³J_{HH} = 3.0 and 1.5 Hz), 6.21, 6.06 (3H total, 2:1 integration, overlapping t's and t, Tp 4-position), 5.63 (1H, β-furyl CH bound, d, ³J_{HH} = 3 Hz), 1.30 (9H, PMe₃, d, ³J_{HP} = 9 Hz). ¹³C{¹H} NMR (CDCl₃, δ): 205.2 (CO, d, ²J_{CP} = 19 Hz), 180.1 (1C, ipso-furyl, d, ²J_{CP} = 16 Hz), 143.7, 143.6, 143.3, 135.4, 135.2, 134.4 (each a s, Tp 3- and 5-position), 115.2 (α-furyl, s), 110.0 (β-furyl, s), 105.6 (β-furyl, s), 105.3, 105.2, 105.1 (each a s, Tp 4-position), 17.5 (PMe₃, d, ²J_{CP} = 31 Hz). ³¹P{¹H} NMR (CDCl₃, δ): 14.3 (PMe₃, s). Anal. Calcd for C₁₇H₂₂BN₆O₂PRu(C₄H₈O)_{0.2} (Note: ¹H NMR spectroscopy of the analysis sample revealed 1/5 equivalents of THF per equivalent of complex 6): C, 42.79; H, 4.76; N, 16.81. Found: C, 42.34; H, 4.75; N, 16.59.

Catalytic Reactions of Furan with Ethylene Using TpRu(CO)(NCMe)(2-furyl) (1). The procedures for all catalytic reactions were analogous. A representative example is given: Under an atmosphere of dinitrogen, TpRu(CO)(NCMe)(2-furyl) (1) (0.073 g, 0.162 mmol) was added to a high-pressure reaction tube containing furan (1.2 mL, 16.2 mmol), decane (0.31 mL, 1.62 mmol), and mesitylene (5 mL). The reaction vessel was sealed, removed from the glovebox, and placed under 20 psi of ethylene pressure. The resulting solution was submerged in an oil bath (120 °C) equipped with digital temperature regulation. Product formation was monitored periodically using analysis with a GC FID (and compared to an authentic sample 2-ethylfuran purchased from a commercial vendor). Prior to analysis using GC FID, the reaction mixture was cooled in an ice water bath for 15 min. Aliquots were removed using a syringe under a light purge of dinitrogen. Product quantities were determined using integrated ratios of the peaks due to 2-ethylfuran and the internal standard decane. A series of five known standards were prepared consisting of 3:1, 2:1, 1:1, 1:2, and 1:3 molar ratios of decane:2-ethyl furan. A plot of the peak area ratios versus molar ratios gave a regression line. The slope is 2.5 ($R^2 = 0.96$).

Catalytic Reactions of Thiophene with Ethylene Using TpRu(CO)(NCMe)(2-thienyl) (2). Under an atmosphere of dinitrogen, a thick-walled high-pressure reaction tube was charged with TpRu(CO)(NCMe)(2-thienyl) (2) (0.040 g, 0.087 mmol), thiophene (6.9 mL, 87 mmol), and decane (0.17 mL, 0.87 mmol) as an internal standard. The reaction vessel was placed under 40 psi of ethylene pressure and submerged in a hot oil bath (90 °C) equipped with digital temperature regulation. The formation of 2-ethylthiophene was monitored by GC-FID analysis. Prior to analysis using GC FID, the reaction mixture was cooled in an ice water bath for 15 min. Aliquots were removed using a syringe under a light purge of dinitrogen. Product yields were determined using integrated areas of 2-ethylthiophene versus the internal standard decane. A series of five known standards were prepared consisting of 3:1, 2:1, 1:1, 1:2, and 1:3 molar ratios of decane:2-ethylthiophene. A plot of the peak area ratios versus molar ratios gave a regression line. The slope is 1.6 with $R^2 = 0.99$.

Kinetic Study of Acetonitrile Ligand Exchange for TpRu(NCMe)(CO)(Ph). TpRu(NCMe)(CO)(Ph) (0.020 g, 0.043 mmol) was placed in a screw-cap NMR tube and taken up in CD₃CN (0.6 mL). A ¹H NMR spectrum of the solution was

acquired. The tube was placed into a hot oil bath (70 °C), and the ligand exchange reaction was monitored versus time. Every 45 min, the solution was removed from the oil bath and cooled in a solution of ice water, and a ¹H NMR spectrum was acquired. The disappearance of the resonance for bound acetonitrile was monitored relative to the peak area of Tp resonances. The decreased intensity of the resonance due to coordinated acetonitrile and increased intensity of the resonance due to free acetonitrile were the only observed changes in the NMR spectra.

Kinetic Study of Acetonitrile Ligand Exchange for TpRu(NCMe)(CO)(2-furyl) (1). TpRu(NCMe)(CO)(2-furyl) (1) (0.019, 0.043 mmol) was placed in a screw-cap NMR tube and taken up in CD₃CN (0.6 mL). A ¹H NMR spectrum was acquired. The tube was placed into a hot oil bath (70 °C), and the progress of acetonitrile exchange was monitored versus time. Every 90 min, the solution was cooled in an ice bath, and a ¹H NMR spectrum was acquired. The disappearance of the resonance for bound acetonitrile was monitored relative to the peak area of Tp resonances. The decreased intensity of the resonance due to coordinated acetonitrile and increased intensity of the resonance due to free acetonitrile were the only observed changes in the NMR spectra.

Kinetic Study of Acetonitrile Ligand Exchange for TpRu(NCMe)(CO)(2-thienyl) (2). TpRu(NCMe)(CO)(2-thienyl) (2) (0.020, 0.042 mmol) was placed in a screw-cap NMR tube and taken up in acetonitrile-*d*₃ (0.6 mL). The solution was heated to 70 °C for approximately 28 h. A ¹H NMR spectrum was periodically acquired. Prior to data acquisition, the reaction solution tube was cooled in an ice bath. The disappearance of the resonance for bound acetonitrile was monitored relative to the peak area of Tp resonances. The decreased intensity of the resonance due to coordinated acetonitrile and increased intensity of the resonance due to free acetonitrile were the only observed changes in the NMR spectra.

Attempted Isomerization of TpRu(NCMe)(CO)(2-furyl) (1). Representative experiment: In a glovebox under dinitrogen atmosphere, a reaction tube was prepared with TpRu(NCMe)(CO)(2-furyl) (1) (0.201 g, 0.045 mmol), furan (0.10 mL, 1.3 mmol), and 5 mL of THF. This vessel was removed from the glovebox and placed into a hot oil bath (90–100 °C) for 144 h. The reaction solution was cooled to room temperature, and volatiles were removed under reduced pressure. A ¹H NMR spectrum of the resulting solid revealed the quantitative recovery of TpRu(NCMe)(CO)(2-furyl) (1).

X-ray Diffraction Study of TpRu(CO)(NCMe)(2-thienyl) (2) and [TpRu(CO)(μ-C,S-2-thienyl)]₂ (4). The same general procedures were used to perform the X-ray crystallographic analyses of complexes 2 and 4. A suitable crystal was covered in perfluoropolyether (PFO-XR75, Lancaster) and sealed under nitrogen in a glass capillary. The crystal was optically aligned on the four-circle of a Siemens P4 diffractometer equipped with a graphite monochromatic crystal, a Mo Kα radiation source (λ = 0.71073 Å), and a SMART CCD detector held at 5.084 cm from the crystal. Four sets of 20 frames each were collected using the ω scan method and with a 10 s exposure time. Integration of these frames followed by reflection indexing and least-squares refinement produced a crystal orientation matrix and a lattice. Data collection consisted of the measurement of a total of 1650 frames in five different runs covering a hemisphere of data. The program SMART (version 5.6) was used for diffractometer control, frame scans, indexing, orientation matrix calculations, least-squares refinement of cell parameters, and the data collection.⁷⁷ All 1650 crystallographic raw data frames were read by the program SAINT (version 5/6.0) and integrated using

(77) SMART, SAINT, and XPREP programs are part of Bruker AXS crystallographic software package for single-crystal data collection, reduction, and preparation.

3D profiling algorithms. The resulting data were reduced to produce a total of 12 921 reflections (complex **2**) or 5678 reflections (complex **4**) and their intensities and estimated standard deviations. An absorption correction was applied using the SADABS routine available in SAINT. The data were corrected for Lorentz and polarization effects as well as any crystal decay. Data preparation was carried out by using the program XPREP, which gave 4367 unique reflections ($R_{\text{int}} = 3.83\%$) with indices $-12 \leq h \leq 13$, $-15 \leq k \leq 15$, $-19 < l \leq 20$ for complex **2** and gave 3607 unique reflections ($R_{\text{int}} = 0.0391$) with indices $-10 \leq h \leq 11$, $-12 \leq k \leq 11$, $-11 \leq l \leq 13$ for complex **4**. The monoclinic space group was determined to be $P2_1/n$, which is a nonstandard setting of the space group $P2_1/c$ (No. 14). The structure was solved by a combination of direct methods and Fourier methods with the use of SHELX-TL6.1.⁷⁸ Idealized positions for the hydrogen atoms were included as fixed contributions using a riding model with isotropic temperature factors set at 1.2 (aromatic protons) or 1.5 (methyl protons) times that of the adjacent carbon. The position of the B–H proton was refined with a fixed isotropic temperature factor set at 1.2 times that of the boron atom. The positions of the methyl hydrogen atoms were optimized by a rigid rotating group refinement with idealized tetrahedral angles. For complex **2**, the 2-thienyl ligand suffered from a 70:30 two-site disorder, with the two orientations of the planar five-membered ring differing by a nearly 180° rotation around the Ru–C(13) bond axis. The five non-hydrogen atoms within each of these ring orientations were refined anisotropically with the S(1)–C(13) and S(1)–C(16) bonds restrained to 1.68 ± 0.04 Å, the C(14)–C(15) bond restrained to 1.45 ± 0.04 Å, and the C(13)–C(14) and C(15)–(16) bonds restrained to 1.38 ± 0.04 Å. For complex **4**, the dimeric structure is constrained by a crystallographic center of inversion. Full-matrix least-squares refinement, based upon the minimization of $\sum w_i |F_o^2 - F_c^2|^2$, with $w_i^{-1} = [\sigma^2(F_o^2) + (aP)^2 + bP]$, where $a = 0.0436$,

(78) Sheldrick, G. M., *SHELXTL6.1*, Crystallographic software package; Bruker AXS, Inc.: Madison, WI, 2000.

$b = 0.3172$ for complex **2**; $a = 0.0473$, $b = 0.0$ for complex **4**; $P = (\text{Max}(F_o^2, 0) + 2F_c^2)/3$, converged to give the final discrepancy indices. A correction for secondary extinction was not applied. The maximum and minimum residual electron density peaks in the final difference Fourier map were 0.462 and -0.403 e/Å³ for complex **2** and 0.680 and -0.479 e/Å³ for complex **4**, respectively. The linear absorption coefficient, atomic scattering factors, and anomalous dispersion corrections were calculated from values from the International Tables for X-ray Crystallography.⁷⁹

Acknowledgment. T.R.C. acknowledges the Office of Energy Sciences, Office of Science, United States Department of Energy, for support of this research through Grant No. DE-FG02-97ER14811. T.B.G. acknowledges the Office of Energy Sciences, Office of Science, United States Department of Energy, for support of this research through Grant No. DE-FG02-03ER15490, the Alfred P. Sloan Foundation (Research Fellowship), and Bayer Corporation for donation of GC FID instrumentation.

Supporting Information Available: Complete tables of crystal data, collection and refinement data, atomic coordinates, bond distances and angles, and anisotropic displacement coefficients for TpRu(CO)(NCMe)(2-thienyl) (**2**) and [TpRu(CO)(μ -C,S-2-thienyl)]₂ (**4**). Details of the synthesis and characterization of TpRu(CO)(NCMe)(Cl) and TpRu(CO)(NCMe)(2-pyridyl), chart depicting NOEs for the thienyl ligand of TpRu(CO)(NCMe)(2-thienyl) (**2**), representative kinetic plots for acetonitrile exchange reactions, and Cartesian coordinates and structures for all optimized minima. This material is available free of charge via the Internet at <http://pubs.acs.org>.

OM049508R

(79) *International Tables for X-ray Crystallography*; Kynoch Press: Birmingham, 1974; Vol. IV, p 55 (present distributor, D. Reidel, Dordrecht).